doi.org/10.36721/PJPS/2026.40.16420.1

Hesperidin improves motor and sensory recovery and modulates the balance of pro- and anti-inflammatory cytokine profiles after contusive spinal cord injury in mice

Shengli Ma[1] and Zhiliang Yan[2]*

[1]Department of Spinal Cord Injury Rehabilitation, Shaanxi Provincial Rehabilitation Hospital, Xian, Shaanxi, 710000, China
[2]Department of Orthopedic, Xi'an People's Hospital, Xian, Shaanxi, 710000, China

Abstract: **Background**: Hesperidin (HES) has anti-inflammatory and antioxidant properties, but coordinated *in vivo* evidence linking HES to functional recovery, cytokine rebalancing, microglial activation and MAPK signaling after contusive spinal cord injury (SCI) remains limited. **Objectives**: To evaluate whether HES improves motor and sensory function after SCI and to characterize associated changes in the spinal inflammatory microenvironment, oxidative stress and ERK/JNK-MAPK signaling. **Methods**: SCI was induced by a modified Allen weight-drop contusion at T10 in 100 C57BL/6 mice randomly assigned to sham, SCI, or HES low-, medium- and high-dose groups (25, 50 and 100 mg/kg; n = 20 each). HES was administered by gavage once daily for 21 days beginning 2 h after injury. Motor and sensory outcomes were assessed by BMS scoring and mechanical and thermal tests; spinal cord cytokines, redox indices and neurorepair-related factors were measured by ELISA/biochemical assays, microglial activation by Iba1 immunohistochemistry and MAPK phosphorylation by western blotting. **Results**: On day 21, significant functional improvement was observed in the 100 mg/kg group ($p < 0.05$), whereas lower doses showed non-significant trends. In day-7 spinal cord tissue, HES reduced pro-inflammatory cytokines and increased anti-inflammatory cytokines; TNF-α decreased from 218.17 ± 28.11 to 54.39 ± 11.37 pg/mg in the high-dose group ($p < 0.05$). MDA levels were lower, whereas SOD, GSH-Px and CAT activities and T-AOC were higher than in the SCI group ($p < 0.05$). HES also reduced Iba1-positive microglia and ERK1/2 and JNK phosphorylation without altering total ERK1/2 or JNK levels. **Conclusion**: HES was associated with improved motor and sensory recovery, a less inflammatory cytokine profile, attenuated oxidative stress and microglial activation and reduced ERK/JNK phosphorylation after contusive SCI; pathway-specific experiments remain necessary to establish causality.

Keywords: Hesperidin; Inflammatory microenvironment; MAPK signaling pathway; Microglia; Neuroprotection; Spinal cord injury

Submitted 12-03-2026 – Revised 22-04-2026 – Accepted 13-05-2026

Article in Press

INTRODUCTION

Spinal cord injury (SCI) is a major cause of long-term neurological disabilities. Recent epidemiological estimates have reported an annual incidence of acute SCI of approximately 60.6 per million and a lifetime disability rate of approximately 85% (Eli *et al.*, 2021). SCI often results in lasting disability and markedly impairs daily functioning and quality of life (Zhang *et al.*, 2021). Following primary mechanical insult, secondary tissue responses evolve over days to weeks and coincide with persistent deficits in motor control and sensory processing (Kong *et al.*, 2025; Singh *et al.*, 2024). MAPK signaling is one of the pathways activated after injury and is positioned to regulate inflammatory and stress-responsive programs in the damaged cord.

Despite advances in perioperative care and rehabilitation, curative therapies for SCI remain elusive. Surgical decompression and high-dose steroid pulse therapy may provide limited benefits within a narrow therapeutic window while also carrying risks of serious systemic adverse effects (Kaniuk *et al.*, 2025; Khachatryan *et al.*, 2022). Therefore, safe neuroprotective agents capable of acting on multiple targets within the secondary injury cascade are needed. Hesperidin (HES), a natural dihydroflavone glycoside widely present in citrus species, has been shown to have anti-inflammatory, antioxidant, immunomodulatory and anti-apoptotic activities (Pyrzynska, 2022). It also has a favorable safety profile and has been reported to cross the blood–spinal cord barrier (Lee *et al*., 2020). HES has shown neuroprotective effects in several central nervous system disease models, including cerebral ischemia and neurodegenerative disorders (Buzdagli *et al.*, 2023; Fang *et al.*, 2025). Notably, few preclinical studies HES and its metabolite hesperetin in SCI: Liu *et al*. (2023) demonstrated that hesperetin ameliorates SCI via Nrf2-mediated inhibition of pyroptosis, while Raguraman *et al*. (2024) showed that HES promotes neural regeneration in vitro (Liu *et al.*, 2023; Raguraman *et al.*, 2024). These studies suggest that HES-related compounds may influence several components of secondary SCI, but the existing evidence

*Corresponding author: e-mail: yanzhiliangm3@163.com

remains fragmented. The available SCI literature has mainly emphasized either Nrf2-related pyroptosis inhibition or *in-vitro* neural regeneration, whereas the relationship among behavioral recovery, spinal cytokine balance, microglial activation and stress-responsive kinase signaling has not been examined specifically for HES (Liu *et al*., 2023; Raguraman *et al.*, 2024). This distinction is important because secondary SCI is not driven by a single molecular event. Inflammatory cytokine imbalance, microglial activation, oxidative stress, mitochondrial dysfunction and regulated cell death programs form an interdependent injury network that affects both motor and sensory outcomes.

In this context, ERK/JNK-MAPK signaling was prioritized not because ferroptosis, apoptosis, or autophagy are unimportant, but because it offered a more integrated and experimentally tractable readout for the outcome structure of the present study. In this context, ERK/JNK-MAPK signaling was selected as a focused stress- and inflammation-related axis, not as a substitute for assessing apoptosis, ferroptosis or autophagy. Because MAPK signaling may act upstream of, downstream of or parallel to these regulated cell death programs, reduced ERK/JNK phosphorylation cannot exclude their involvement in HES-mediated neuroprotection (Huang *et al*., 2024). Thus, the present data support a candidate MAPK-related pharmacodynamic association, whereas direct causality requires pathway-specific markers and rescue experiments. Recent studies further support this inflammatory signaling perspective in SCI: obacunone improved functional recovery by attenuating TLR4/MyD88/p38-MAPK-mediated neuroinflammation, low-intensity pulsed ultrasound promoted recovery by regulating microglia-mediated neuroinflammation and kakkalide improved SCI repair by shifting microglia toward a reparative M2-like phenotype through SIRT3-dependent mitophagy (Kuang *et al*., 2026; Li *et al*., 2026; You *et al*., 2026). Meanwhile, recent review-level evidence indicates that apoptosis, ferroptosis, autophagy and necroptosis are interconnected downstream injury programs in SCI rather than mutually exclusive linear mechanisms (Zeng and Zeng, 2026). Accordingly, the present study did not regard MAPK signaling as the sole mechanism of HES action. Instead, ERK/JNK-MAPK was selected as a focused pharmacodynamic axis linking the known anti-inflammatory and antioxidant properties of HES with the observed cytokine, microglial, oxidative stress and behavioral outcomes.

In this study, an SCI model was established in C57BL/6 mice using the Allen's impact method (Wang *et al.*, 2025). This study evaluated the effects of HES on the recovery of motor and sensory motor and sensory function, characterized changes in the inflammatory microenvironment and oxidative stress within injured spinal cord tissue and examined the involvement of the MAPK pathway. The goal was to provide experimental support for HES as a natural candidate for SCI interventions. Notably, while the anti-inflammatory and antioxidant properties of HES have been reported in other neural injury models, most previous studies focused on isolated endpoints and did not systematically link HES-mediated modulation of the MAPK pathway to simultaneous improvements in both motor and sensory function in the context of contusive SCI. This study fills this gap by providing a comprehensive evaluation of HES effects across behavioral, histopathological, biochemical and molecular domains, establishing a coherent association between MAPK signaling attenuation and modulation of the spinal inflammatory microenvironmen.

MATERIALS AND METHODS

Experimental animals

A total of 100 SPF-grade male C57BL/6 mice (6–8 weeks old, 20–22 g) were obtained from Nantong Jingqi Biotechnology Co., Ltd. (license SYXK (Su) 2023-0028). Animals were housed under controlled conditions (22±2 °C, 55±5% humidity, 12 h light/dark cycle) with ad libitum access to food and water and were acclimatized for 7 days before the experiments. All animal procedures were approved by the Institutional Animal Ethics Committee (No. IACUC2023355) and conducted in accordance with the relevant guidelines. Before allocation, animals were screened according to prespecified inclusion and exclusion criteria.

Inclusion criteria

Mice were eligible if they were SPF-grade male C57BL/6 mice aged 6-8 weeks, weighed 20-22 g and showed normal activity, grooming and feeding after the 7-day acclimatization period.

Exclusion criteria

Animals were excluded before randomization if they showed overt illness, abnormal behaviour, marked body-weight loss during acclimatization, skin lesions, limb dysfunction, or death before model establishment. After surgery, animals or data points were excluded only if moderate contusion could not be confirmed intraoperatively, comparable initial neurological deficit was not verified at 24 h after SCI, a humane endpoint was reached before the scheduled assessment, or a documented technical failure occurred during sample processing or assay measurement.

Animal grouping and drug administration

Mice were randomized into five groups (n = 20 each) using a random number table: Sham, SCI and HES low-, medium- and high-dose groups. Sample size was determined based on previous similar SCI studies (Ge *et al*., 2021) and power analysis (power = 0.8, $\alpha = 0.05$) showing n = 10 per endpoint provides sufficient statistical

Article in Press

power to detect biologically meaningful differences. The primary outcome used for sample-size determination was the POD21 BMS locomotor score, which was prespecified as the main functional endpoint for evaluating neurological recovery after contusive SCI. Allocation concealment was achieved using sequentially numbered, sealed opaque envelopes prepared by an investigator not involved in the study. HES (Sigma-Aldrich, purity ≥98%) was suspended in 0.5% CMC-Na (Sigma-Aldrich) and administered by gavage once daily for 21 days starting 2 h after injury. The doses were 25, 50 and 100 mg/kg, respectively; Sham and SCI mice received the same volume of vehicle. These doses were selected based on previous preclinical studies demonstrating neuroprotective effects of HES in central nervous system injury models (Lim *et al*., 2022; Liu *et al*., 2023), where 25–100 mg/kg oral administration showed dose-dependent efficacy without observable systemic toxicity. Preliminary pilot experiments further confirmed that doses below 25 mg/kg had no significant neuroprotective effects, while doses above 100 mg/kg did not provide additional benefits in locomotor recovery. Pharmacokinetic studies in rodents have shown that oral HES has a bioavailability of approximately 12–20%, with a plasma half-life of 4–6 h and accumulates in neural tissue at concentrations sufficient to exert biological effects (Pyrzynska, 2022). The once-daily dosing regimen for 21 days was selected to maintain sustained therapeutic levels throughout the critical secondary injury phase of SCI. After the initial group allocation, mice within each group were further randomly assigned by an independent investigator, using a random number table, to either the day-7 tissue collection subgroup (n = 10) or the day-21 behavioral/sensory assessment subgroup (n = 10); subgroup allocation was concealed from the investigators responsible for outcome assessment. No animals died unexpectedly, reached a humane endpoint before the scheduled endpoint, or were excluded from the final analyses. Therefore, all allocated animals were included in the analysis. Behavioral and sensory outcomes were analysed using n = 10 mice per group on POD21. ELISA, biochemical assays, histopathology and Iba1 immunohistochemistry were performed using n = 10 biological samples per group on POD7, unless otherwise stated. Western blotting was performed using n = 6 independent biological samples per group.

Establishment of the mouse SCI model

SCI was induced using a modified Allen weight-drop contusion at the T10 level (Wang *et al*., 2025). After anesthesia with 3% pentobarbital sodium (Sigma-Aldrich, 40 mg/kg, i.p.), T9–T10 laminectomy was performed to expose the T10 spinal cord while keeping the dura intact. In the injured groups, a 10 g rod was dropped from the exposed cord (2.5 cm) to create a moderate contusion. Successful injury was initially confirmed intraoperatively by immediate hemorrhagic swelling at the impact site and a transient tail-flick/tail-swing response; in addition, BMS scoring was performed 24 h after SCI by a blinded investigator to verify comparable initial neurological deficits across the injured groups before treatment-related recovery was interpreted. Postoperatively, the mice received penicillin (200,000 U/mouse, i.p.) once daily for 3 days and bladder expression was performed twice daily until spontaneous voiding returned.

Motor and sensory function assessment

BMS locomotor scoring was performed on POD 1, 3, 7, 14 and 21 to monitor the recovery trajectory, whereas the inclined plane, grid-walking, rotarod, footprint, von Frey, hot-plate and cold-plate tests were performed on POD 21 as endpoint functional and sensory assessments. Hindlimb locomotion was scored using the Basso Mouse Scale (BMS; 0–9) (Ge *et al.*, 2021), with scoring based on joint movement, coordination, trunk stability, paw placement and weight support. Balance was assessed using the standard inclined plane test: each mouse was placed on a rubber-covered board, the angle was increased in 5° increments and the maximal angle at which the mouse maintained its position for 5 s was recorded as the inclined-plane angle. All behavioral and sensory assessments were performed under standardized conditions (constant temperature 22±2 °C, dim lighting and quiet environment) between 9:00 AM and 12:00 PM to minimize circadian variation and all tests were conducted by a single investigator who was blinded to the group assignments. Skilled stepping was examined using a grid-walking apparatus by counting the hindlimb slips during locomotion. Endurance and coordination were evaluated using a rotarod and the latency to fall was recorded at a constant rotation speed. Gait was further characterized by footprint analysis to obtain hindlimb stride length (Shanghai Yuyan Scientific Instrument Co., Ltd.). The sensory testing was conducted in parallel. Before testing, all mice were acclimatized to the testing environment for 30 min daily for 3 consecutive days, followed by a 15-min acclimatization period immediately before each test session. For von Frey filament testing, each mouse received 5 trials per filament with a 5-min interval between trials and the mechanical threshold was calculated using the up-down method as previously described. For hot plate and cold plate tests, each mouse was tested 3 times with a 10-min interval between trials and the final withdrawal latency was defined as the average of the 3 trials. A cutoff time of 30 s was set for both thermal tests to prevent tissue damage. Mechanical sensitivity was assessed using von Frey filaments and was recorded as the minimal force (g) eliciting a withdrawal response. Thermal sensitivity was measured using a hot plate set at 55±0.5 °C and a cold plate set at 4±0.5 °C and paw withdrawal or licking latency was recorded. Mechanical allodynia was evaluated using the up–down method.

Article in Press

Animal euthanasia and humane endpoints

Mice were euthanized on POD7 for tissue collection or after POD21 behavioral testing. Euthanasia was performed in a non-prefilled chamber using 100% CO_2 at a gradual displacement rate of 30–70% of chamber volume/min. CO_2 exposure was maintained for at least 1 min after respiratory arrest, followed by cervical dislocation. Death was confirmed by absence of breathing, heartbeat and pedal reflex. Animals reaching humane endpoints, including severe weight loss, infection, autophagia or moribund status, were euthanized immediately. Expected postoperative events after SCI included transient hindlimb dysfunction and temporary bladder dysfunction, which were managed by routine postoperative care and twice-daily bladder expression until spontaneous voiding returned. No unexpected adverse events, procedure-related deaths, severe infection, autophagia, or early humane-endpoint euthanasia occurred before the planned POD7 or POD21 endpoints.

Sample collection and processing

Day 7 was selected for tissue analysis because it corresponds to the peak of inflammatory response and microglial activation in the contusive SCI model (Hellenbrand *et al*., 2021), while day 21 was chosen for behavioral assessment as it represents a stable time point for evaluating long-term functional recovery in mice (Ge *et al*., 2021). Spinal cord segments T8–T11 were collected and briefly rinsed with ice-cold PBS to remove residual blood. Each specimen was divided for downstream analyses. One portion was fixed in 4% paraformaldehyde for 24 h, processed by dehydration and clearing, embedded in paraffin and sectioned at 4 μm for histology and immunohistochemistry. The remaining portion was snap-frozen in liquid nitrogen and stored at −80 °C for ELISA/biochemical assays and western blotting.

Measurement of inflammatory cytokines and neurorepair-related factors

The frozen spinal cord tissue was processed to obtain a clear supernatant for analysis. Proinflammatory cytokines (TNF-α, IL-1β, IL-6, IL-17 and IFN-γ), anti-inflammatory cytokines (IL-10, IL-4, TGF-β1 and IL-13), neurorepair-related factors (BDNF, NGF and GAP-43) and redox indices [malondialdehyde (MDA), superoxide dismutase (SOD), glutathione peroxidase (GSH-Px), catalase (CAT) and total antioxidant capacity (T-AOC)] were measured in the tissue supernatant. Briefly, frozen spinal cord tissue was homogenized in ice-cold RIPA buffer (1:10 tissue-to-buffer ratio, w/v) supplemented with a complete protease inhibitor cocktail (Roche, 11836170001) using a glass homogenizer. The homogenate was centrifuged at 12,000 rpm for 15 min at 4 °C and the clear supernatant was collected for analysis. These analytes were quantified using commercially available mouse ELISA kits from Wuhan Huamei Bioengineering Co., Ltd., according to the manufacturer's instructions. All samples were assayed in duplicate and an assay was accepted only when the standard curve met the manufacturer's linearity criteria, duplicate coefficients of variation were <10% and blank controls remained below the lower detection limit. The reported intra-assay and inter-assay coefficients of variation were <8% and <10%, respectively, with detection limits ranging from 1.0 to 10.0 pg/mL for cytokines. Because these kits were not independently cross-validated against another supplier, cytokine concentrations were interpreted as internally controlled comparative measurements rather than absolute reference values. Inter-observer reliability for behavioral testing was confirmed by a second blinded investigator scoring 20% of randomly selected animals, with an intraclass correlation coefficient (ICC) of 0.92 for BMS scores.

Histopathological semi-quantification and microglial activation

Paraffin sections (4 μm) were deparaffinized and stained with hematoxylin and eosin to evaluate tissue morphology. Microglial activation was assessed by Iba1 immunohistochemistry using a DAB chromogenic readout after pH 6.0 citrate antigen retrieval and sections were counterstained with hematoxylin to identify nucleated cells. Histopathological semi-quantification was conducted in a blinded manner, focusing on inflammatory cell infiltration and tissue necrosis (Servicebio Technology Co. Ltd.). All slides were coded with random numbers to conceal group identities and the same blinded investigator performed all quantitative analyses using ImageJ software (National Institutes of Health). For Iba1 quantification, five non-overlapping fields per section were selected at 400× magnification and Iba1-positive cells were expressed as the percentage of hematoxylin-counterstained nucleated cells in the same field. Using a 0–3 semi-quantitative scoring scale: 0 = no abnormality; 1 = mild inflammatory infiltration and focal necrosis involving <25% of the spinal cord cross-sectional area; 2 = moderate inflammatory infiltration and necrosis involving 25–50% of the area; 3 = severe inflammatory infiltration and extensive necrosis involving >50% of the area.

Western blot analysis of MAPK pathway-related proteins

Frozen spinal cord tissue was lysed in RIPA buffer (Beyotime Biotechnology Co., Ltd.) supplemented with phenylmethylsulfonyl fluoride (PMSF, 1 mM), a complete protease inhibitor cocktail (Roche, 11836170001) and a phosphatase inhibitor cocktail (Roche, 04906837001) on ice for 30 min and clarified by centrifugation (12,000 rpm, 15 min, 4 °C). The protein concentration was measured using a BCA assay (Beyotime Biotechnology Co., Ltd.). Equal amounts of protein were separated by SDS-PAGE (Beyotime Biotechnology Co., Ltd.) and transferred to PVDF membranes (MilliporeSigma). After blocking with 5% non-fat milk (BD Biosciences) for 2 h at room temperature.

Article in Press

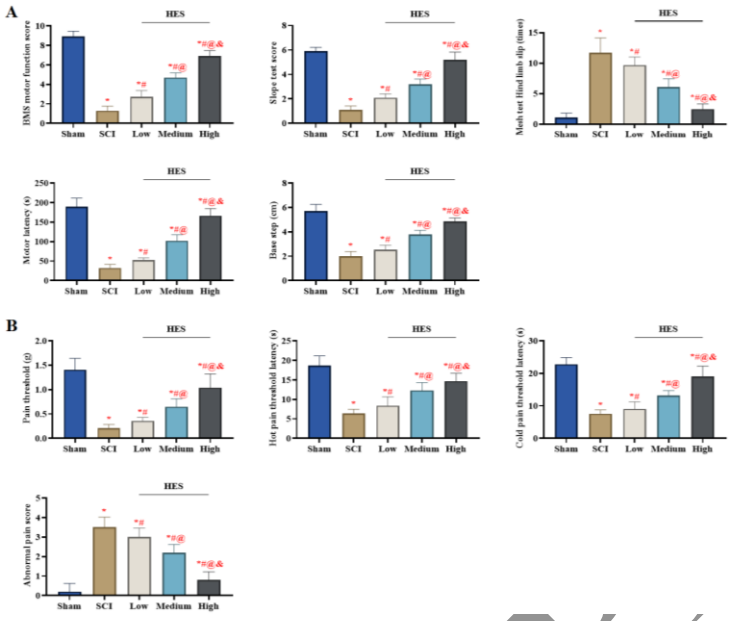


Fig. 1: Hesperidin improves locomotor recovery and alleviates pain-related hypersensitivity after SCI. (A) Motor function outcomes on postoperative day 21, including BMS locomotor score, inclined-plane maximal angle, hindlimb slips in the mesh test, rotarod latency, and base step length; (B) Sensory function outcomes on postoperative day 21, including mechanical pain threshold, hot-plate withdrawal latency, cold-plate withdrawal latency and abnormal pain score. * means $p < 0.05$ compared with sham group, # means $p < 0.05$ compared with SCI group, @ means $p < 0.05$ compared with HES-low dose group and & means $p < 0.05$ compared with HES-medium dose group.

The membranes were incubated overnight at 4 °C with the following primary antibodies: anti-ERK1/2 (Abcam, ab184699, rabbit monoclonal, 1:1000), anti-phospho-ERK1/2 (Thr202/Tyr204) (Abcam, ab214036, rabbit monoclonal, 1:1000), anti-JNK (Abcam, ab179461, rabbit monoclonal, 1:1000), anti-phospho-JNK (Thr183/Tyr185) (Abcam, ab124956, rabbit monoclonal, 1:1000) and anti-GAPDH (Abcam, ab8245, mouse monoclonal, 1:5000). The membranes were washed in TBST (Beyotime Biotechnology Co., Ltd.) and incubated with horseradish peroxidase-conjugated secondary antibody (1:5000, Jackson Immuno Research Laboratories, Inc.) for 2 h at room temperature. Bands were visualized by chemiluminescence and quantified using the ImageJ software. Phosphorylated proteins were normalized to their corresponding total protein levels and GAPDH served as the loading control. All western blot experiments were performed using 6 independent biological samples per group and each experiment was repeated 3 times to ensure reproducibility.

Statistical analysis

The experimental unit was an individual mouse across all allocation, treatment, behavioral, histopathological, biochemical and molecular outcome assessments. SPSS 26.0 (IBM Corp., Armonk, NY, USA) was used for statistical analysis. Data distribution and homogeneity of variance were assessed using the Shapiro–Wilk and Levene tests. Normally distributed continuous variables are presented as mean ± SD and were compared using one-way ANOVA followed by Tukey's HSD test. Ordinal variables, including BMS and histopathological scores and non-normally distributed variables are presented as median (IQR) and were analysed using the Kruskal–Wallis test followed by Dunn's post-hoc test with Bonferroni correction. Statistical significance was defined as a two-sided *p*-value of <0.05.

RESULTS

Effects of HES on motor and sensory function in SCI mice

Serial BMS assessment showed comparable initial deficits at 24 h after SCI and progressive locomotor improvement over time, with the most evident between-group separation observed on POD21; at this endpoint, the SCI group showed lower locomotor scores and poorer performance in balance and coordination tasks than the sham group. At 24 h after SCI, BMS scores were comparable among the SCI, HES-low, HES-medium and HES-high groups ($p > 0.05$), indicating similar initial injury severity before treatment-related functional differences were evaluated. The stride length was reduced and the stepping errors on the grid increased. Sensory testing also differed from sham, with reduced mechanical thresholds and shorter withdrawal latencies on hot and cold plates ($p < 0.05$). After HES administration, the readouts improved. The 100 mg/kg group showed the highest BMS scores compared with the SCI group when analysed as ordinal data ($p < 0.05$) and sensory indices improved in the same direction (Fig. 1).

Article in Press

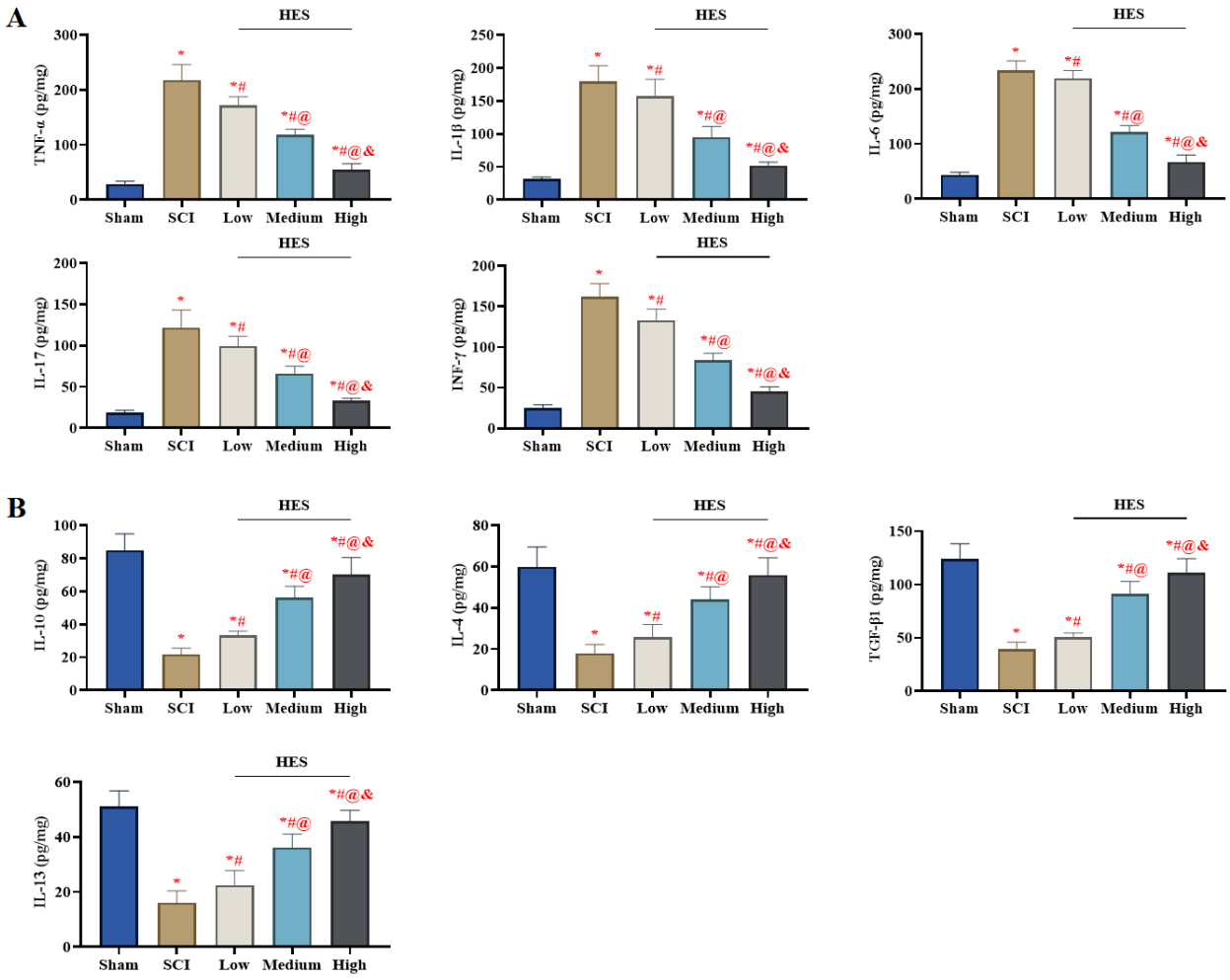


Fig. 2: Hesperidin rebalances the inflammatory cytokine profile in injured spinal cord tissue after SCI. (A) Pro-inflammatory cytokines in spinal cord tissue (TNF-α, IL-1β, IL-6, IL-17 and IFN-γ); (B) Anti-inflammatory cytokines in spinal cord tissue (IL-10, IL-4, TGF-β1 and IL-13). * means $p < 0.05$ compared with sham group, # means $p < 0.05$ compared with SCI group, @ means $p < 0.05$ compared with HES-low dose group and & means $p < 0.05$ compared with HES-medium dose group.

Bidirectional regulation of inflammatory cytokine profiles by HES in injured spinal cord tissue

SCI was associated with a cytokine profile dominated by proinflammatory mediators. TNF-α, IL-1β, IL-6, IL-17 and IFN-γ increased relative to the sham group, whereas IL-10, IL-4, TGF-β1 and IL-13 decreased (all $p < 0.05$). With HES treatment, this imbalance was partially reversed; pro-inflammatory cytokines declined as the dose increased and anti-inflammatory cytokines recovered. At 100 mg/kg, TNF-α decreased from 218.17 ± 28.11 pg/mg to 54.39 ± 11.37 pg/mg ($p < 0.05$), accompanied by restoration of TGF-β1 (Fig. 2).

Regulation of oxidative stress levels in spinal cord tissue by HES in SCI mice

Oxidative stress markers are also altered after SCI. Compared with the sham group, MDA increased, while SOD, GSH-Px, CAT and T-AOC decreased ($p < 0.05$). HES moves these indices in opposite directions. MDA levels were lower and antioxidant capacity was higher in the 100 mg/kg group than in the SCI group ($p < 0.05$) (Fig. 3).

Effects of HES on neurorepair-related factors in spinal cord tissue of SCI mice

In the SCI group, BDNF, NGF and GAP-43 levels were lower than those in the sham group ($p < 0.05$). HES increased all three factors, with the high-dose group recovering to more than 85% of sham levels ($p < 0.05$) (Fig. 4).

Effects of HES on histopathological injury and microglial activation in spinal cord tissue of SCI mice

H&E sections from the sham group showed preserved tissue architecture without obvious cavitation, whereas the SCI group displayed tissue disruption with necrosis and cavity formation accompanied by inflammatory cell infiltration.

Article

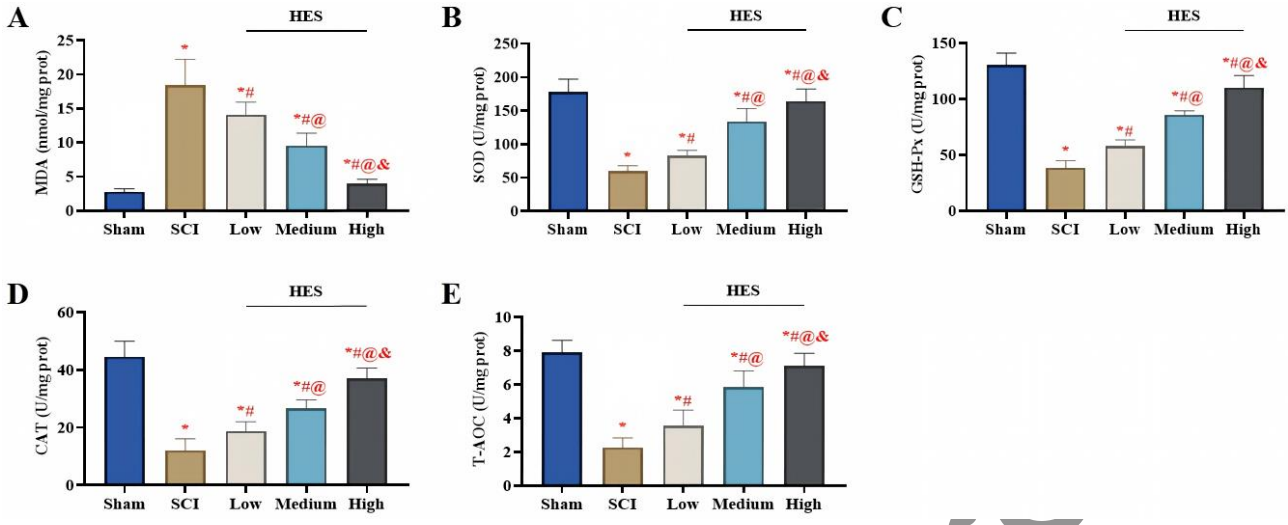


Fig. 3: Hesperidin attenuates oxidative stress and restores antioxidant capacity in spinal cord tissue after SCI. The levels of (A) MDA, (B) SOD, (C) GSH-Px, (D) CAT and (E) T-AOC were measured. * means $p < 0.05$ compared with sham group, # means $p < 0.05$ compared with SCI group, @ means $p < 0.05$ compared with HES-low dose group and & means $p < 0.05$ compared with HES-medium dose group.

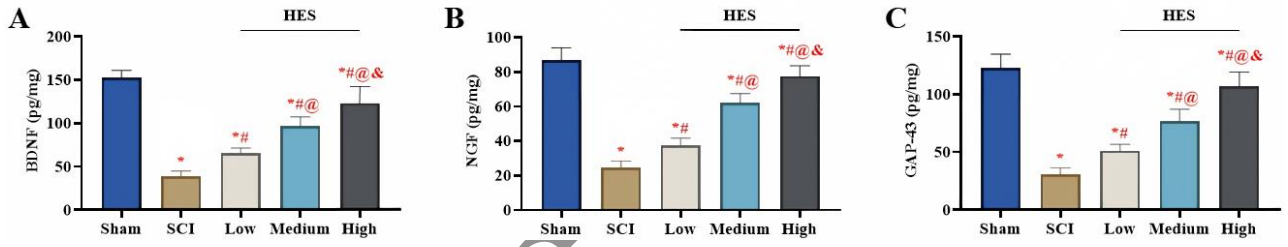


Fig. 4: Hesperidin enhances neurorepair-associated factors in spinal cord tissue after SCI. The levels of (A) BDNF, (B) NGF and (C) GAP-43 were measured. * means $p < 0.05$ compared with sham group, # means $p < 0.05$ compared with SCI group, @ means $p < 0.05$ compared with HES-low dose group and & means $p < 0.05$ compared with HES-medium dose group.

Iba1 immunostaining showed a higher proportion of activated microglia in the SCI group than in the sham group ($p < 0.05$). HES treatment reduced the extent of these pathological findings. In the 100 mg/kg group, the cavity area ratio decreased to (8.58±0.76)% ($p < 0.05$) and both the Iba1-positive cell proportion and ordinal histopathological scores for inflammatory infiltration and tissue necrosis were lower than those in the SCI group after non-parametric analysis ($p < 0.05$) (Fig. 5).

Regulation of the MAPK signaling pathway in spinal cord tissue by HES in SCI mice

ERK1/2 and JNK signaling was evaluated by measuring the total protein levels and phosphorylation ratios in spinal cord extracts. Total ERK1/2 and JNK levels did not differ significantly among the groups ($p > 0.05$). In contrast, p-ERK1/2/ERK1/2 and p-JNK/JNK increased after SCI compared to the sham group ($p < 0.05$). HES reduced both phosphorylation ratios, with the largest reduction observed in the high-dose group (>70% vs. SCI group, $p < 0.05$). Notably, the reduction in phosphorylation ratios showed low intra-group variability (coefficient of variation <15% in all groups), indicating a consistent association between HES treatment and attenuation of excessive MAPK pathway activation (Fig. 6).

Overall, a consistent dose-dependent relationship was observed across all measured parameters, including motor and sensory function scores, inflammatory cytokine levels, oxidative stress indices, neurorepair factor expression, histopathological scores and MAPK phosphorylation ratios. In all cases, high-dose HES (100 mg/kg) produced the most pronounced effects, followed by medium-dose (50 mg/kg) and low-dose (25 mg/kg) HES, with statistically significant differences between consecutive dose groups for most primary endpoints.

DISCUSSION

In this contusion SCI model, HES improved locomotor performance and alleviated sensory hypersensitivity.

Article Pre

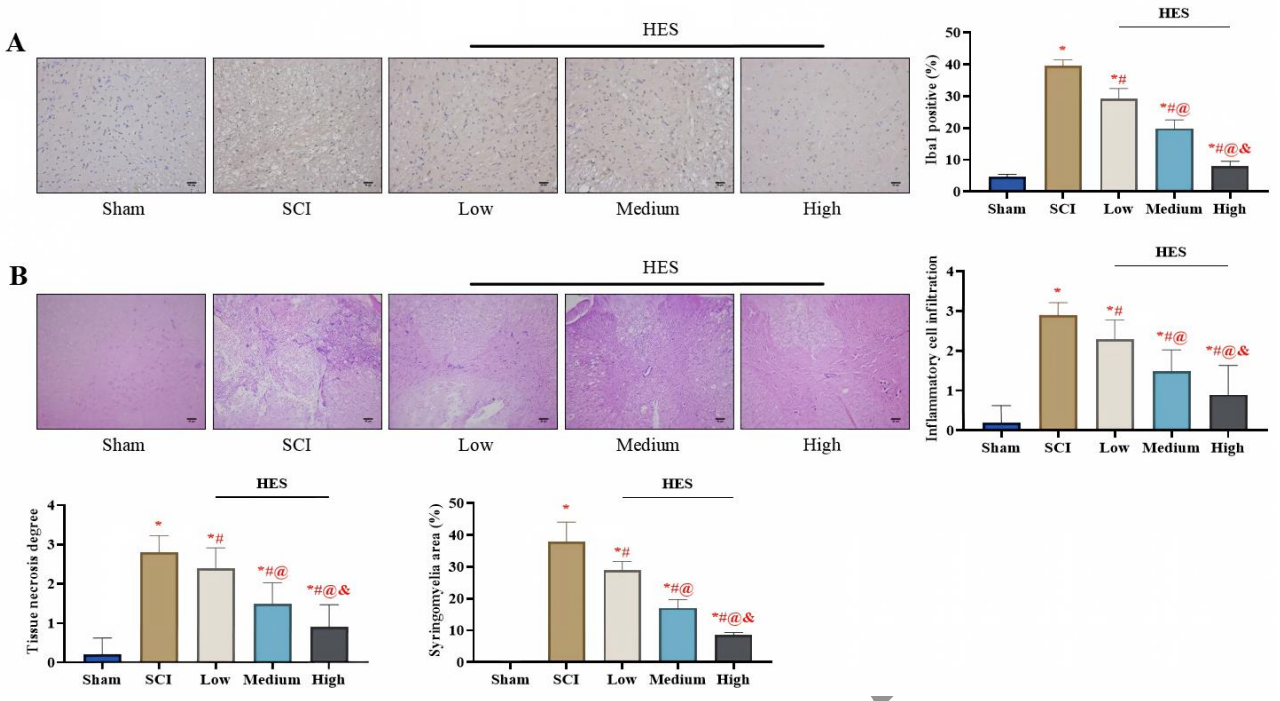


Fig. 5: Hesperidin reduces microglial activation and mitigates histopathological injury after SCI. (A) Representative Iba1 immunohistochemistry images across groups and quantitative analysis of Iba1-positive cells (%); (B) Representative H & E-stained sections and semi-quantitative evaluation (including inflammatory cell infiltration score, tissue necrosis degree and syringomyelia/cavity area (%)). Scale bars as indicated. * means $p < 0.05$ compared with sham group, # means $p < 0.05$ compared with SCI group, @ means $p < 0.05$ compared with HES-low dose group and & means $p < 0.05$ compared with HES-medium dose group.

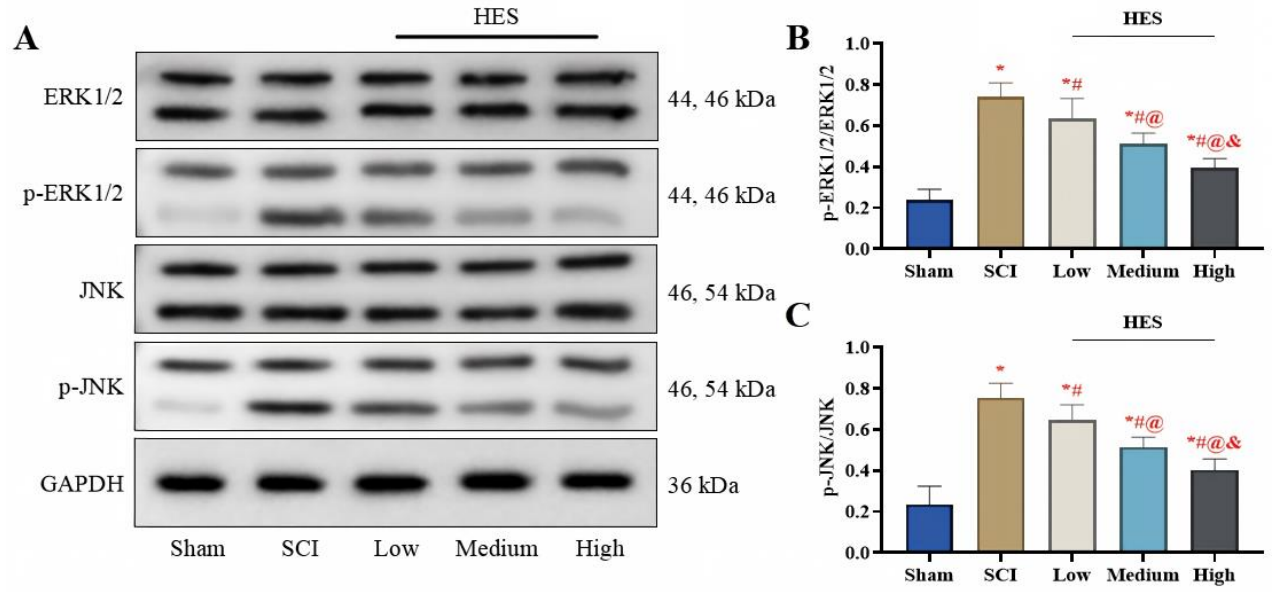


Fig. 6: Hesperidin suppresses excessive MAPK pathway activation in spinal cord tissue after SCI. Representative (A) Western blot of ERK1/2, p-ERK1/2, JNK, p-JNK and GAPDH, GAPDH was used as a loading control; (B, C) Quantitative analysis of phosphorylation levels relative to total protein: (B) p-ERK1/2/ERK1/2 ratio and (C) p-JNK/JNK ratio. * means $p < 0.05$ compared with sham group, # means $p < 0.05$ compared with SCI group, @ means $p < 0.05$ compared with HES-low dose group and & means $p < 0.05$ compared with HES-medium dose group.

These behavioral changes were accompanied by a cytokine shift toward a less inflammatory profile, reduced oxidative stress, fewer Iba1-positive microglia, increased neurorepair-related factors and lower ERK1/2 and JNK phosphorylation. These findings support an association between HES-mediated functional improvement and attenuation of inflammatory and stress-responsive molecular changes after SCI. However, the present design does not prove a direct causal sequence from MAPK inhibition to cytokine rebalancing or neurological recovery. Therefore, the MAPK-related findings should be interpreted as a biologically plausible signaling correlate rather than definitive mechanistic evidence. A conservative working interpretation is that HES treatment may reduce excessive ERK/JNK activation in parallel with decreased microglial activation and a more favorable inflammatory cytokine profile, thereby contributing to a tissue environment that is more permissive for neurological recovery.

Neurological recovery is the central endpoint of SCI intervention and remains the focus of preclinical research (Widerstrom-Noga, 2023). In the present study, high-dose HES improved locomotor capacity, balance/coordination and gait recovery while also attenuating mechanical hypersensitivity and abnormal thermal responses. This combined improvement in motor and sensory outcomes suggests that HES may act on multiple components of the secondary injury cascade. Previous studies have shown that HES improves motor coordination in cerebral ischemia–reperfusion models and reduces neuropathic pain in sciatic nerve injury models (Keskin *et al.*, 2025; Wang *et al.*, 2023). Building on these findings, the current results extend comparable motor and sensory improvements to the SCI setting, thus strengthening the functional rationale for HES in neural injury. Liu *et al*. (2023) reported that hesperetin improved SCI outcomes mainly through Nrf2-mediated inhibition of NLRP3 inflammasome activation and pyroptosis, providing important evidence for an antioxidant-pyroptosis axis. Raguraman *et al*. further supported the regenerative potential of HES in an in-vitro composite-based neural regeneration model, but that design did not address systemic dosing, contusive SCI pathology, behavioral recovery, or *in-vivo* inflammatory signaling (Raguraman *et al*., 2024). Compared with previous studies on HES and its metabolite hesperetin in SCI, the present study uniquely demonstrates simultaneous improvements in both motor and sensory function and establishes a coherent association between these functional benefits and modulation of the ERK/JNK-MAPK pathway.

In the present dataset, the day-7 spinal cord profile in SCI mice favored pro-inflammatory signaling: TNF-α and IL-1β were elevated, whereas IL-10 and TGF-β1 were lower than in the Sham group. HES shifted these measures in the opposite direction and simultaneously reduced Iba1-positive microglia in the injured region. Together, these findings indicate the attenuation of inflammatory activation in the injured cord after HES treatment (Liu *et al*., 2021). However, the current experiments do not distinguish whether HES acts directly on microglia (Hellenbrand *et al*., 2021) or indirectly through upstream changes in tissue injury and redox stress (Abd Elmaaboud *et al.*, 2023); both remain plausible in the context of contusion SCI.

MAPK readouts provide a biochemical correlation for these tissue changes (Liu *et al*., 2022; Huang *et al*., 2024; Lin *et al.*, 2025). SCI increased ERK1/2 and JNK phosphorylation, whereas the total ERK1/2 and JNK levels did not differ among the groups. After HES treatment, both phosphorylation ratios decreased and the high-dose group showed reductions exceeding 70%, relative to SCI. This change was observed at the level of phosphorylation rather than the total protein abundance, suggesting modulation of pathway activation. Whether this MAPK change is required for cytokine and microglial effects cannot be concluded from the present design and would require direct testing with pathway inhibitors or genetic approaches (Lim *et al*., 2022; Abd Elaleem *et al*., 2025). This limitation is particularly relevant because MAPK activation may function either upstream of cytokine production or as a downstream response to tissue injury, oxidative stress and glial activation (Huang *et al*., 2024; Lin *et al*., 2025; Zeng and Zeng, 2025). Accordingly, the observed decrease in ERK/JNK phosphorylation should not be interpreted as proof that MAPK inhibition is the primary mechanism of HES. Instead, it identifies ERK/JNK-MAPK signaling as a candidate pathway that warrants direct validation in future studies using pharmacological blockade, genetic manipulation, or time-course analyses. The focus on ERK/JNK-MAPK should therefore be interpreted in comparison with, rather than in opposition to, other secondary injury mechanisms. Ferroptosis, apoptosis and autophagy are highly relevant to neuronal survival, glial responses and tissue preservation after SCI, but the present study did not include iron metabolism markers, caspase activation assays, LC3/p62 flux analysis, or pathway-specific rescue experiments. These mechanisms therefore cannot be excluded as contributors to the protective effects of HES. The current data support a narrower conclusion: HES treatment was associated with suppression of excessive stress-responsive MAPK phosphorylation and rebalancing of the inflammatory microenvironment, while its effects on defined cell death programs require direct validation in subsequent mechanistic studies (Zeng and Zeng, 2026).

This study has several limitations. First, only a moderate contusion model was used, whereas clinical SCI included diverse injury patterns, such as transection, compression and ischemia (Barbiellini Amidei *et al.*, 2022); validation

Article in Press

across additional models is important for generalizability. Second, the outcomes were assessed up to postoperative day 21 and long-term functional recovery and safety with prolonged administration were not evaluated. Third, although MAPK signaling was associated with HES protection, pathway-specific inhibitors or genetic approaches were not used for reverse validation. Fourth, this study did not include a clinically used neuroprotective agent as a positive comparator, which limits direct comparison of therapeutic efficacy. Methylprednisolone, the only FDA-approved drug for acute SCI, has significant systemic side effects and narrow therapeutic window and its clinical use remains controversial. Future head-to-head studies comparing HES with standard-of-care agents will be needed to further define its translational potential. Finally, microglial activation was assessed using Iba1, a general microglial marker that does not distinguish between pro-inflammatory (M1) and anti-inflammatory (M2) phenotypes. Future studies using double immunofluorescence staining for M1/M2-specific markers will be needed to further characterize the effects of HES on microglial polarization. Additionally, some intra-group variability was observed in behavioral and biochemical measurements, which is common in preclinical SCI studies due to inherent biological variation in injury severity and individual animal responses. However, the consistent dose-dependent effects across multiple independent endpoints and the statistically significant differences between groups support the robustness of these conclusions.

CONCLUSION

HES improved motor and sensory outcomes after SCI in mice and was accompanied by reduced microglial activation, rebalanced inflammatory cytokines, attenuated oxidative stress, increased neurorepair-related factors and lower ERK1/2 and JNK phosphorylation. These results suggest that HES may help reshape the inflammatory microenvironment after contusive SCI and identify ERK/JNK-MAPK signaling as a candidate pathway associated with this effect. However, pathway-specific experiments are still required to confirm whether MAPK modulation is necessary for the observed neuroprotective benefits.

Acknowledgments
None.

Authors' contributions
Shengli Ma conceived and designed the project and wrote the paper. Zhiliang Yan generated the data and analyzed the data. Shengli Ma and Zhiliang Yan modified the manuscript. All authors gave final approval of the version to be published.

Funding
There was no funding.

Data availability statement
The datasets generated during and/or analysed during the current study are available from the corresponding author on reasonable request.

Ethical approval
The study was approved by the Institutional Animal Ethics Committee (No. IACUC2023355) and conducted in accordance with the relevant guidelines. All animal handling, experimental procedures and manuscript reporting were carried out in compliance with the ARRIVE (Animal Research: Reporting of *In vivo* Experiments) guidelines. This study was performed in adherence with the ARRIVE guidelines. See supplementary file for the ARRIVE checklist.

Conflict of interest
All the authors declare no conflict of interest.

REFERENCES

Abd Elaleem WS, Ghaiad HR, Abd Elmawla MA and Shaheen AA (2025). Attenuation of p38 MAPK/NF-kappaB/TRPV1/CGRP is involved in the antinociceptive effect of hesperidin methyl chalcone and taxifolin in paclitaxel-induced peripheral neuropathy. *BioFactors.*, **51**(1): e2125.

Abd Elmaaboud MA, Estfanous RS, Atef A, Kabel AM, Alnemari KA, Naguib TM, Alsufyani SE, Darwish HW and Arab HH (2023). Dapagliflozin/hesperidin combination mitigates lipopolysaccharide-induced Alzheimer's disease in rats. *Pharmaceuticals (Basel)*, **16**(10): 1370.

Barbiellini Amidei C, Salmaso L, Bellio S, Trevisan C and Saia M (2022). Epidemiology of traumatic spinal cord injury: A large population-based study. *Spinal. Cord.*, **60**(9): 812-819.

Buzdagli Y, Eyipinar CD, Kaci FN and Tekin AH (2023). Effects of hesperidin on anti-inflammatory and antioxidant response in healthy people: A meta-analysis and meta-regression. *Int. J. Environ. Health. Res.*, **33**(12): 1390-1405.

Eli I, Lerner DP and Ghogawala Z (2021). Acute traumatic spinal cord injury. *Neurol. Clin.*, **39**(2): 471-488.

Fang L, Yang T, Nijiati Y, Shahanati D, Abudukeremu A, Li J, Shi W, Maimaitiyiming D and Aikemu A (2025). Multi-omics analyses reveal that hesperidin ameliorates high-altitude pulmonary hypertension by restoring gut-lung axis homeostasis. *Phytomedicine.*, **145**: 157069.

Ge MH, Tian H, Mao L, Li DY, Lin JQ, Hu HS, Huang SC, Zhang CJ and Mei XF (2021). Zinc attenuates ferroptosis and promotes functional recovery in contusion spinal cord injury by activating Nrf2/GPX4 defense pathway. *CNS. Neurosci. Ther.*, **27**(9): 1023-1040.

Hellenbrand DJ, Quinn CM, Piper ZJ, Morehouse CN,

Article in Press

Fixel JA and Hanna AS (2021). Inflammation after spinal cord injury: A review of the critical timeline of signaling cues and cellular infiltration. *J. Neuroinflammation.*, **18**(1): 284.

Huang S, Zhang Y, Shu H, Liu W, Zhou X and Zhou X (2024). Advances of the MAPK pathway in the treatment of spinal cord injury. *CNS. Neurosci. Ther.*, **30**(6): e14807.

Kaniuk JK, Kumar D, Tennyson J, Hurka KL, Margolis A, Bucaloiu A, Selner A and Ahuja CS (2025). Spinal cord injury remyelination: Pathways to therapies. *Int. J. Mol. Sci.*, **26**(15): 7249.

Keskin E, Yilmaz B and Gel MS (2025). Neuroprotective effects of hesperidin on cerebral vasospasm after subarachnoid hemorrhage in rats: An experimental study. *Ulus. Travma. Acil. Cerrahi. Derg.*, **31**(12): 1157-1167.

Khachatryan Z, Haunschild J, von Aspern K, Borger MA and Etz CD (2022). Ischemic spinal cord injury-experimental evidence and evolution of protective measures. *Ann. Thorac. Surg.*, **113**(5): 1692-1702.

Kong G, Liu J, Wang J, Yu X, Li C, Deng M, Liu M, Wang S, Tang C, Xiong W and Fan J (2025). Engineered extracellular vesicles modified by angiopep-2 peptide promote targeted repair of spinal cord injury and brain inflammation. *ACS. Nano.*, **19**(4): 4582-4600.

Kuang W, Zhang M, Zhang J, Huang H, Chen Q, Yu C, Peng B, Sun W, Lin J, Cheng J and Zhu L (2026). Obacunone promotes functional recovery after spinal cord injury by attenuating neuroinflammation by targeting the TLR4/MyD88/p38 MAPK pathway. *Drug. Des. Devel. Ther.*, **20**: 577707.

Lee BK, Hyun SW and Jung YS (2020). Yuzu and hesperidin ameliorate blood-brain barrier disruption during hypoxia via antioxidant activity. *Antioxidants (Basel).*, **9**(9): 843.

Li X, Liu Y, Liu W, Wang T, Shang H, Zhong H, Deng Z, Zhou X and Wei X (2026). Low-intensity pulsed ultrasound promotes spinal cord injury recovery by regulating microglia-mediated neuroinflammation. *CNS. Neurosci. Ther.*, **32**(4): e70849.

Lim C, Zhen AX, Ok S, Fernando P, Herath H, Piao MJ, Kang KA and Hyun JW (2022). Hesperidin protects SH-SY5Y neuronal cells against high glucose-induced apoptosis via regulation of MAPK signaling. *Antioxidants (Basel)*, **11**(9): 1707.

Lin FX, Gu HY and He W (2025). MAPK signaling pathway in spinal cord injury: Mechanisms and therapeutic potential. *Exp. Neurol.*, **383**: 115043.

Liu C, Hu F, Jiao G, Guo Y, Zhou P, Zhang Y, Zhang Z, Yi J, You Y, Li Z, Wang H and Zhang X (2022). Dental pulp stem cell-derived exosomes suppress M1 macrophage polarization through the ROS-MAPK-NFkappaB P65 signaling pathway after spinal cord injury. *J. Nanobiotechnology.*, **20**(1): 65.

Liu X, Zhang Y, Wang Y and Qian T (2021). Inflammatory response to spinal cord injury and its treatment. *World Neurosurg*, **155**: 19-31.

Liu Z, Tu K, Zou P, Liao C, Ding R, Huang Z, Huang Z, Yao X, Chen J and Zhang Z (2023). Hesperetin ameliorates spinal cord injury by inhibiting NLRP3 inflammasome activation and pyroptosis through enhancing Nrf2 signaling. *Int. Immunopharmacol.*, **118**: 110103.

Pyrzynska K (2022). Hesperidin: A review on extraction methods, stability and biological activities. *Nutrients.*, **14**(12): 2387.

Raguraman M, Zhou X, Mickymaray S, Alothaim AS and Rajan M (2024). Hesperidin guided injured spinal cord neural regeneration with a combination of MWCNT-collagen-hyaluronic acid composite: *In-vitro* analysis. *Int. J. Pharm.*, **650**: 123609.

Singh G, Sharma P, Forrest G, Harkema S, Behrman A and Gerasimenko Y (2024). Spinal cord transcutaneous stimulation in cervical spinal cord injury: A review examining upper extremity neuromotor control, recovery mechanisms and future directions. *J. Neurotrauma.*, **41**(17-18): 2056-2074.

Wang Y, Li C, Xing J, Zhu Y, Sun M, Yin S, Liu J, Zou L, Liang S and Liu S (2023). Neohesperidin alleviates the neuropathic pain behavior of rats by downregulating the P2X4 receptor. *Neurochem. Res.*, **48**(3): 781-790.

Wang Z, Zhang Y, Liu W, Liu K, Wang S, Jing R and Cong M (2025). GDF11 alleviates spinal cord injury in rats by modulating microglia polarization through Smad2/3 and MAPK/NFkappaB signaling pathways. *Int. Immunopharmacol.*, **163**: 115197.

Widerstrom-Noga E (2023). Neuropathic pain and spinal cord injury: Management, phenotypes and biomarkers. *Drugs.*, **83**(11): 1001-1025.

You T, Dai B, Ding X, He Z, Peng J, Tao S, Ye L, Song T, Fan Z and Chen N (2026). Kakkalide promotes spinal cord injury repair by regulating microglial M2 polarization via mitophagy. *Phytomedicine.*, **153**: 157985.

Zeng W and Zeng F (2026). Endoplasmic reticulum stress-mediated cell death in spinal cord injury: From molecular mechanisms to therapeutic applications. *Front. Cell. Dev. Biol.*, **14**: 1742297.

Zeng WC and Zeng FJ (2025). Regulatory effect of inflammatory mediators in spinal cord injury. *Front. Immunol.*, **16**: 1619337.

Zhang Y, Al Mamun A, Yuan Y, Lu Q, Xiong J, Yang S, Wu C, Wu Y and Wang J (2021). Acute spinal cord injury: Pathophysiology and pharmacological intervention (Review). *Mol. Med. Rep.*, **23**(6): 417.

Article in Press